

## Supporting Information for

### Controllable Organic Magnetoresistance in Polyaniline Coated Poly(*p*-phenylene-2,6-benzobisoxazole) Short Fibers

Hongbo Gu,<sup>\*a</sup> Xiaojiang Xu,<sup>a</sup> Jingyi Cai,<sup>a</sup> Suying Wei,<sup>\*b</sup> Huige Wei,<sup>b,c</sup> Hu Liu,<sup>d,f</sup>

David P. Young,<sup>e</sup> Qian Shao,<sup>h</sup> Shide Wu,<sup>g</sup> Tao Ding,<sup>d</sup> and Zhanhu Guo,<sup>\*d</sup>

<sup>a</sup>Shanghai Key Lab of Chemical Assessment and Sustainability,  
School of Chemical Science and Engineering, Tongji University, Shanghai 200092,  
People's Republic of China

<sup>b</sup>Department of Chemistry & Biochemistry, Lamar University, Beaumont, TX, 77710  
USA

<sup>c</sup>College of Chemical Engineering and Materials Science, Tianjin University of Science  
and Technology, Tianjin 300457, China

<sup>d</sup>Integrated Composites Lab (ICL), Department of Chemical & Biomolecular Engineering  
University of Tennessee, Knoxville, TN, 37966, USA

<sup>e</sup>Department of Physics and Astronomy, Louisiana State University, Baton Rouge,  
Louisiana 70803, USA

<sup>f</sup>Key Laboratory of Materials Processing and Mold (Zhengzhou University), Ministry of  
Education, National Engineering Research Center for Advanced Polymer Processing  
Technology, Zhengzhou University, Zhengzhou, China

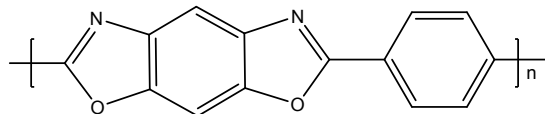
<sup>g</sup>Henan Provincial Key Laboratory of Surface and Interface Science, Zhengzhou  
University of Light Industry, No. 136, Science Avenue, Zhengzhou, 450001, China

<sup>h</sup>College of Chemical and Environmental Engineering, Shandong University of Science  
and Technology, Qingdao, Shandong 266590, China

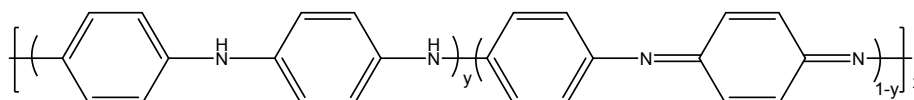
\*Corresponding author

E-mail: [hongbogu2014@tongji.edu.cn](mailto:hongbogu2014@tongji.edu.cn); [suying.wei@lamar.edu](mailto:suying.wei@lamar.edu); [zguo10@utk.edu](mailto:zguo10@utk.edu)

### Chemical structure of PBO:



### Chemical structure of PANI:



## Experimental Section

**Materials.** Aniline ( $C_6H_7N$ ), ammonium persulfate (APS,  $(NH_4)_2S_2O_8$ ), and *p*-toluene sulfonic acid (PTSA,  $C_7H_8O_3S$ ) were purchased from Sigma Aldrich. Nitric acid (68.0-70.0 wt%) was obtained from Fisher Scientific. Zylon (PBO short fibers) was provided by Toyobo Co., Ltd. All the chemicals were used as-received without any further purification.

**Preparation of Acid Treated PBO (t-PBO).** PBO short fibers (1.0 g) were oxidized in 100 mL concentrated nitric acid (68.0-70.0 wt%) by mechanical stirring at 50 °C in the water bath for one and half hours. After that, deionized water was used to wash the filtrate until pH was about 7. Then the acid treated PBO (t-PBO) was dried in a vacuum oven at 80 °C overnight.

**Fabrication of PANI coated t-PBO short fibers.** The PANI coated PBO short fibers were prepared via a facile surface initiated polymerization (SIP) method. Briefly, t-PBO (0.0881-2.511 g) were added into 90 mL deionized water under mechanical stirring (SCIOLOGEX OS20-Pro LCD Digital Overhead Stirrer, 300 rpm) combined with sonication (Branson 8510). The aniline (18 mmol) was dropped into the above solution

using syringe. Then this mixed solution was maintained for 1 h in an ice-water bath. After that, the PTSA (15 mmol) and APS (9 mmol) solution (in 35 mL deionized water) were mixed with the above solution and mechanically stirred and sonicated continuously for additional 1 h in the ice-water bath for further polymerization. The product was vacuum filtered and repeatedly washed with deionized water. The precipitant was further washed with 1 mol L<sup>-1</sup> PTSA. The obtained final dark green PBO/PANI nanocomposites were dried at 60 °C in a traditional oven overnight. The PBO/PANI nanocomposites with a fiber loading of 5, 10, 30 and 60 wt% were synthesized. The as-received PBO fibers without acid treatment were prepared for PANI nanocomposites and pure PANI was also fabricated following the above procedure for comparison.

**Characterizations.** Fourier transform infrared spectroscopy (FTIR) coupled with an ATR accessory (Bruker Inc. Vector 22) was applied to characterize the chemical structure of the PBO fibers and PANI coated t-PBO fibers in the range of 500 to 4000 cm<sup>-1</sup> at a resolution of 4 cm<sup>-1</sup>. Thermogravimetric analysis (TGA) was conducted by TA instruments TGA Q-500 at a heating rate of 10 °C min<sup>-1</sup> from 30 to 800 °C under an air flow rate of 60 mL min<sup>-1</sup>. The morphology of the PBO/PANI nanocomposites was evaluated using scanning electron microscope (SEM, Hitachi S-3400 scanning electron microscopy). The PANI coated t-PBO fibers were pressed in a form of disc pellet with a diameter of 25 mm by applying a pressure of 50 MPa in a hydraulic presser and the average thickness was about 1.0 mm. The same sample was also used to measure the resistivity ( $\rho$ ) by a standard four-probe method from 100 to 290 K. Magnetoresistance was carried out using a standard four-probe technique by a 9-Tesla Physical Properties Measurement System (PPMS) by Quantum Design at room temperature. The four probes

were 0.002 inch diameter platinum wires, which were attached by silver paste to the sample. Moreover, the magnetic field was applied perpendicular to the current.

### FTIR of PANI

In the FTIR of PANI, The characteristic absorption peaks of pure PANI ( $1550$ ,  $1470$ ,  $1290$ , and  $802\text{ cm}^{-1}$ ), arising from the C=C stretching vibration of the quinoid and benzenoid rings, C-N stretching vibration of the benzenoid unit, and out-of-plane bending of C-H in the substituted benzenoid ring, respectively.

### Scanning electron microscope (SEM)

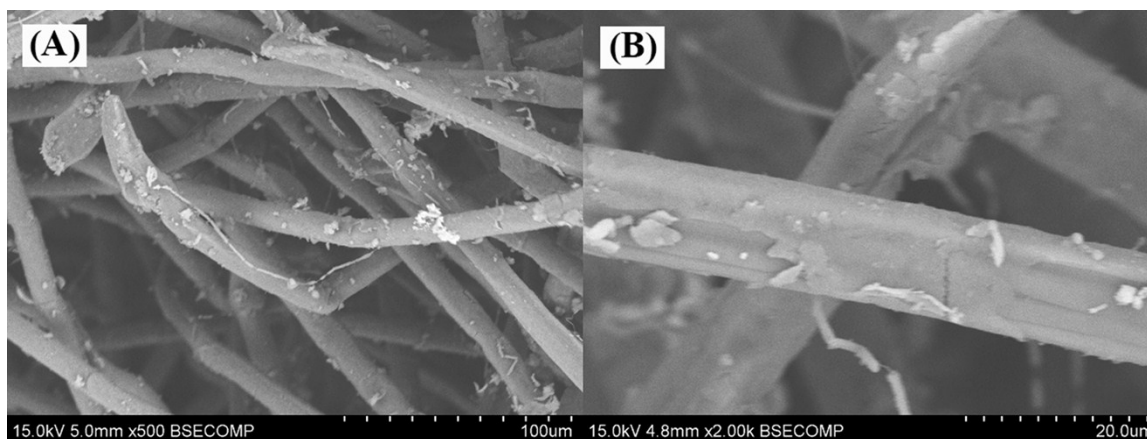


**Fig. S1** SEM images of PANI coated as-received PBO fibers with 60 wt% loading of as-received PBO fibers.

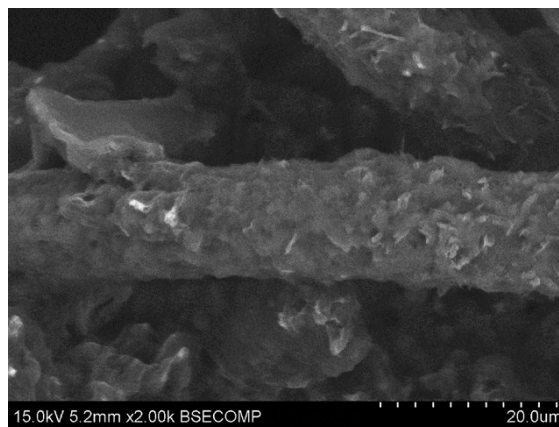


**Fig. S2** SEM image of PANI coated t-PBO fiber with t-PBO loading of 5 wt%.

### Variable range hopping (VRH) mechanism

The variable range hopping (VRH) mechanism is represented as eqn (S1):<sup>29</sup>

$$\sigma = \sigma_0 \exp\left[-\left(\frac{T_0}{T}\right)^{1/n+1}\right] \quad (\text{S1})$$

where the constant  $\sigma_0$  stands for the conductivity at infinite low temperature, which includes tunnelling through the high barrier created by the organic capping layer and accounts for the attempt frequency of charge carriers trying to escape the nanocrystal;  $T$  (K) is the Kelvin temperature and constant  $T_0$  (K) is the Mott characteristic temperature, which is related to the energy needed for the hop of charge carriers. The  $\sigma_0$  and  $T_0$  can be obtained from the intercept and slope in the linear fitting of  $\ln(\sigma) \sim T^{-1/(n+1)}$ .

**Table S1.  $T_0$ ,  $\sigma_0$  and  $\rho_r$  for the PANI coted t-PBO fibers.**

Samples	$T_0 \times 10^3$ (K)	$\sigma_0$ (S cm <sup>-1</sup> )	$\rho_r$
PANI coted t-PBO fibers			
with t-PBO loading of 5 wt%	2.522	5.905	6.787
with t-PBO loading of 10 wt%	5.272	0.412	17.138
with t-PBO loading of 30 wt%	4.198	2.098	11.075
with t-PBO loading of 60 wt%	2.792	$1.799 \times 10^{-3}$	9.299

It is found that the resistance of PANI coated t-PBO fibers with 5 wt% loading of t-PBO fibers is pretty smaller than other samples with the values range of 24.87 ~ 3.84 ohm from 100 to 290 K. And for the 60 wt% loading of PANI coated t-PBO fibers, the resistance is grown dramatically from  $1.12 \times 10^5$  (100 K) to  $1.33 \times 10^4$  ohm (290 K). The value of the resistivity ratio ( $\rho_r$ ,  $\rho_r = \rho_{100} / \rho_{290}$ ) is used to

evaluate the disorder in the PANI wrinkles covered t-PBO fibers and the relevant results are shown in Table S1, in which the  $\rho_r$  is independent of the t-PBO fiber loadings.

### Magnetoresistance

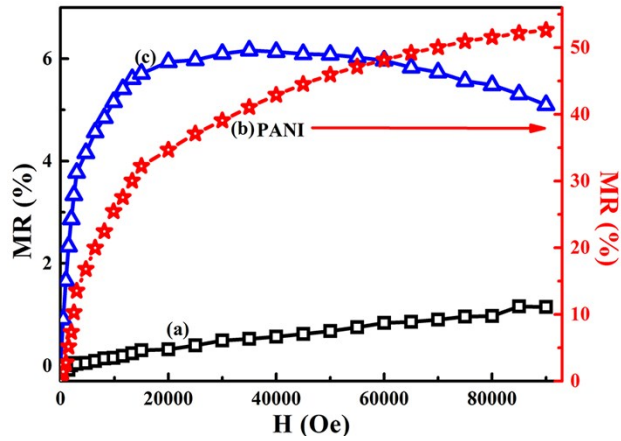


Fig. S3 Room temperature magnetoresistance of the pure PANI, PANI coated t-PBO fibers with t-PBO loading of 5 and 10 wt%, respectively.

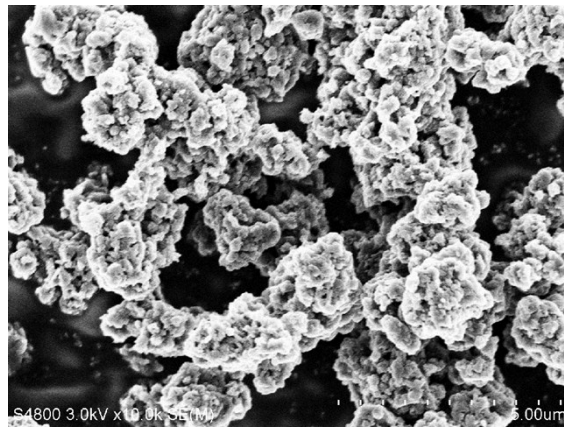
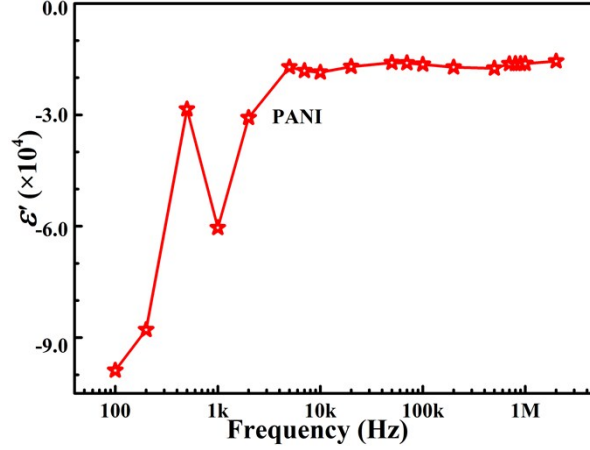


Fig. S4 SEM image of pure PANI.



**Fig. S5** Frequency dependent real permittivity of pure PANI.

### Wave-function Shrinkage Model:

In the wave-function shrinkage model, the contraction of the electronic wave function at impurity centers in a magnetic field has been considered and the  $R(H, T) / R(0, T)$  can be expressed as Eqn (S1):<sup>1</sup>

$$R(H, T) / R(0, T) = \exp\{\xi_C(0)[\xi_C(H) / \xi_C(0) - 1]\} \quad (\text{S1})$$

where  $\xi_C(0) = (T_0 / T)^{1/4}$  for the 3-d Mott VRH electrical conduction mechanism,  $\xi_C(H) / \xi_C(0)$  is the normalized hopping probability parameter and is a function of  $H / P_C$  for the Mott VRH electrical conduction mechanism.  $H$  is the magnetic field,  $P_C$  is the fitting parameter, which is the normalized characteristic magnetic field and can be given by eqn (6) for the 3-dimensional Mott VRH system, Eqn (S2):<sup>2</sup>

$$P_C = 6\hbar / [ea_0^2 (T_0 / T)^{1/4}] \quad (\text{S2})$$

where  $e$  is electron charge,  $\hbar$  is the reduced Planck's constant, and  $T_0$  is the Mott characteristic temperature (K). In the low magnetic field limit, Eqn (S1) is simplified to Eqn (S3):<sup>3</sup>

$$R(H, T) / R(0, T) \approx 1 + t_2 \frac{H^2}{P_C^2} \left( \frac{T_0}{T} \right)^{1/4} \quad (\text{S3})$$

And the MR is defined in Eqn (S4):

$$\text{MR} = \frac{R(H, T) - R(0, T)}{R(0, T)} \approx t_2 \frac{H^2}{P_C^2} \left( \frac{T_0}{T} \right)^{1/4} = t_2 \frac{e^2 a_0^4}{36\hbar^2} \left( \frac{T_0}{T} \right)^{3/4} H^2 \quad (\text{S4})$$

where the numerical constant  $t_2 = 5/2016$ .<sup>2</sup> From Eqn (S4), it can be concluded that the MR value obtained from wave-function shrinkage model is always positive, thus, it is often used to explain the positive MR value. According to Eqn (S4), in wave-function shrinkage model, the localization length  $a_0$  can be expressed from the slope of the curve by plotting  $\text{MR} \sim H^2$  ( $k = t_2 \frac{e^2 a_0^4}{36\hbar^2} \left( \frac{T_0}{T} \right)^{3/4}$ ). The localization length  $a_0$  can be calculated by

Eqn (S5) from  $T_0$ , positive MR value and  $H$ :

$$a_0^4 = \frac{36\hbar^2 \text{MR}}{t_2 e^2} \left( \frac{T_0}{T} \right)^{-3/4} H^{-2} \quad (\text{S5})$$

The obtained localization length  $a_0$  at different  $H$  for the samples with a positive MR value is listed in Table S2.

### Forward Interference Model:

In the forward interference model, the ratio  $R(H, T)/R(0, T)$  caused by the interference effects is described by empirical Eqn (S6), which neglects the quadratic term in  $H$ :<sup>4-6</sup>

$$R(H, T) / R(0, T) \approx 1 / \{1 + C_{\text{sat}} [H / H_{\text{sat}}] / [1 + H / H_{\text{sat}}]\} \quad (\text{S6})$$

where the fitting parameter  $C_{\text{sat}}$  is a constant and the other fitting parameter  $H_{\text{sat}}$  is the



effective magnetic field to saturate the MR. By fitting  $R(H)/R(0) \sim H$  via Eqn (S6) by using Polymath software, the obtained  $C_{\text{sat}}$  value for PANI coated t-PBO fibers with t-PBO loading of 60wt% is 0.0251127.

For the Mott VRH electrical conduction mechanism,  $H_{\text{sat}}$  is given by Eqn (S7):<sup>2</sup>

$$H_{\text{sat}} \approx 0.7 \left( \frac{8}{3} \right)^{3/2} \left( \frac{1}{a_0^2} \right) \left( \frac{h}{e} \right) \left( \frac{T}{T_0} \right)^{3/8} \quad (\text{S7})$$

where  $h$  is Planck's constant,  $e$  is electron charge and  $T_0$  is the Mott characteristic temperature (K). In the low-field limit, Eqn (S6) becomes Eqn (S8):

$$R(H, T) / R(0, T) \approx 1 - C_{\text{sat}} [H / H_{\text{sat}}] \quad (\text{S8})$$

Substituting Eqn (S7) into Eqn (S8) and rearranging, the obtained MR is as Eqn (S9):

$$MR = \frac{\Delta R(H, T) - R(0, T)}{R(0, T)} \approx -C_{\text{sat}} [H / H_{\text{sat}}] = -C_{\text{sat}} \frac{H}{0.7 \left( \frac{8}{3} \right)^{3/2} \left( \frac{1}{a_0^2} \right) \left( \frac{h}{e} \right) \left( \frac{T}{T_0} \right)^{3/8}} \quad (\text{S9})$$

The obtained localization length  $a_0$  at different  $H$  for the samples with the negative MR value is also listed in Table S2.

**Table S2.** Calculated  $a_0$  from wave-function shrinkage model and forward interference model.

Samples	Parameter	Magnetic field $H$ (T)		
		1	5	9
5% t-PBO/PANI	$a_0$ (nm)	0.409	0.263	0.224
10% t-PBO/PANI	$a_0$ (nm)	1.547	0.718	0.536
30% t-PBO/PANI	$a_0$ (nm)	0.857	0.396	0.283

---

60% t-PBO/PANI	$a_0$ (nm)	348.664	622.529	725.550
----------------	------------	---------	---------	---------

---

### References:

1. T.-I. Su, C.-R. Wang, S.-T. Lin and R. Rosenbaum, *Phys. Rev. B*, 2002, **66**, 054438.
2. H. Gu, J. Guo, X. Zhang, Q. He, Y. Huang, H. A. Colorado, N. S. Haldolaarachchige, H. L. Xin, D. P. Young, S. Wei and Z. Guo, *J. Phys. Chem. C*, 2013, **117**, 6426-6436.
3. H. Gu, J. Guo, H. We, Y. Huang, C. Zhao, Y. Li, Q. Wu, N. Haldolaarachchige, D. P. Young, S. Wei and Z. Guo, *Phys. Chem. Chem. Phys.*, 2013, **15**, 10866-10875.
4. U. Sivan, O. Entin-Wohlman and Y. Imry, *Phys. Rev. Lett.*, 1988, **60**, 1566-1569.
5. R. Rosenbaum, A. Milner, S. Hannahs, T. Murphy, E. Palm and B. Brandt, *Physica B*, 2001, **294-295**, 340-342.
6. O. Entin-Wohlman, Y. Imry and U. Sivan, *Phys. Rev. B*, 1989, **40**, 8342-8348.